Final state rescattering effects in axio-hadronic η and η' decays

Daniele S. M. Alves^a Sergi Gonzàlez-Solís^{a,b,c}

^a Theoretical Division, Los Alamos National Laboratory, Los Alamos, NM 87545, U.S.A.

E-mail: spier@lanl.gov, sergig@icc.ub.edu

ABSTRACT: It has been long-understood that final state rescattering effects provide $\mathcal{O}(1)$ corrections to hadronic meson decays rates, such as $\eta \to \pi\pi\pi$ and $\eta' \to \eta\pi\pi$. Hence, one would expect that such effects would be just as important in axio-hadronic η and η' decays, such as $\eta^{(\prime)} \to \pi\pi a$, where a is an axion or axion-like particle (ALP). And indeed they are, as we show in this paper by using the treatment of dispersion relations to include the effects of strong final state interactions in several axio-hadronic processes, namely, $\eta^{(\prime)} \to \pi^0\pi^0 a$, $\eta^{(\prime)} \to \pi^+\pi^- a$, and $\eta' \to \eta\pi^0 a$. We also compute the perturbative, leading order decay rates for multiple ALP emission, such as in $\eta^{(\prime)} \to \pi^0 a a$, $\eta' \to \eta a a$ and $\eta^{(\prime)} \to a a a$, and briefly discuss the expected corrections from strong interactions and the processes that must be considered for an accurate rate estimation of these multi-ALP decay channels.

^bDepartament de Física Quàntica i Astrofísica, Universitat de Barcelona, Martí i Franquès, 1, 08028 Barcelona, Spain

^cInstitut de Ciències del Cosmos, Universitat de Barcelona, Martí i Franquès, 1, 08028 Barcelona, Spain

Contents		
1	Introduction	1
2	 Theoretical framework 2.1 ALP-χPT Lagrangian and leading order decay amplitudes 2.2 Decay kinematics 	3
3	Pion-pion final state interactions with dispersion relations 3.1 Phase shift input and Omnès function	10 12
4	Branching ratios for single ALP channels	15
5	Multi-ALP final states	18
6	Conclusions and Outlook	22

1 Introduction

Axions and axion-like particles (ALPs) are natural and generic predictions of theories beyond the Standard Model (BSM) with spontaneously broken PQ symmetries, and possess incredibly rich phenomenology [1, 2]. In particular, axions/ALPs can couple to quarks, leptons, and gauge bosons, and their masses and decay constants can range over orders of magnitude, from 10^{-22} eV to the Planck scale [3–6]. In this vast parameter space, this class of particles can leave imprints in cosmology [7–10], modify properties of SM particles through virtual corrections [11–19], mediate interactions between matter in the SM and/or in a dark sector [20–22], and be produced in reactions and decays in intensity frontier experiments [23–33], high energy colliders [34–41], and astrophysical environments [42–45].

Much attention has been given in the recent literature to ALPs that couple primarily to electroweak gauge bosons and/or leptons. The phenomenology of such "electroweak ALPs" and "leptonic ALPs" is amenable to perturbative calculations, such that signal predictions are generally accurate and reliable. On the other hand, low energy signals of hadronically-coupled axions and ALPs—and this includes the QCD axion that solves the strong CP problem [46–49]—have been explored to a lesser degree [13, 50–60], in part due to the significant challenges in making accurate predictions. Specifically, the low energy phenomenology of hadronic axions/ALPs is plagued by large uncertainties associated with non-perturbative strong dynamics. While in the 1980s there were some attempts to fold these uncertainties into phenomenological predictions as "fudge" factors [61, 62], this has been largely forgotten in the recent literature, and, to a good approximation, studies of hadronic axion/ALP phenomenology in the past two decades have completely ignored any effects beyond naive leading order in chiral perturbation theory (χ PT).

In this work, we attempt to mitigate this issue in the context of axio-hadronic decays of the η and η' mesons. Unlike other mesons such as Kaons, D, and B mesons—which decay through flavor-violating electroweak interactions—the decay of η and η' mesons is dominated by the strong interactions. Furthermore, any axion or ALP that couples in the ultraviolet (UV) to quarks and/or gluons must be emitted in η and η' decays. This makes these mesons an ideal choice as a first place to investigate the effects of low energy strong dynamics in axion/ALP phenomenology. In addition, the prospect of upcoming η/η' factories¹, such as the Jefferson Lab Eta Factory (JEF) [63] and REDTOP [64], further motivates the investigation of rare $\eta^{(\prime)}$ decays as probes of BSM physics.

We pay special attention to single ALP emission in the $\eta^{(\prime)} \to \pi\pi a$ decay channel. This channel has been previously investigated in the context of the QCD axion using a U(3) chiral effective Lagrangian at leading order [65]. In the framework of Resonance Chiral Theory, ref. [53] went beyond leading order and included nonperturbative effects by means of the exchange of low-lying QCD scalar resonances. Existing literature also includes leading order calculations for a generic gluon-coupled ALPs [52]. Here, we go beyond existing leading order calculations and exploit the universality of the $\pi\pi$ final state interactions (FSI) via dispersion relations (see, e.g. [66–73]) to account for the strong $\pi\pi$ final state rescattering in $\eta^{(\prime)} \to \pi\pi a$ decays. We show that these corrections are significant, and, if neglected, can lead to a major underestimation of axio-hadronic decay rates, almost reaching an order of magnitude for certain regions of ALP parameter space.

We also consider the single ALP channel $\eta' \to \eta \pi^0 a$, albeit with less care for quantifying the uncertainties stemming from the phase shift in the $\eta \pi^0$ final state rescattering.

Finally, we calculate, for the first time, the leading order $\eta^{(\prime)}$ decay rates involving multiple ALP emission, such as $\eta^{(\prime)} \to \pi^0 aa$, $\eta^\prime \to \eta aa$ and $\eta^{(\prime)} \to aaa$, and provide a brief discussion of the magnitude of FSI corrections and the additional processes involved. We leave a complete treatment of FSI effects in multi-ALP decay channels to a future publication.

The structure of this article is as follows. Sec. 2 outlines our theoretical framework, including our notation, leading order ALP-chiral Lagrangian, and derivation of the amplitudes for single ALP $\eta^{(\prime)}$ decays (Sec. 2.1); we end this section by specifying our conventions for decay kinematic variables (Sec. 2.2). The core contribution of this study is found in Sec. 3, where we use the framework of dispersion relations to extract $\pi\pi$ final state interactions effects using the $\pi\pi$ S-wave phase shift (Subsec. 3.1). In Sec. 4 we obtain the branching ratios of single ALP $\eta^{(\prime)}$ decays for two benchmark scenarios, and in Sec. 5 we obtain the leading order amplitudes and decay rates with multiple ALP emission. We summarize our main results and comment on experimental prospects in Sec. 6.

¹The Jefferson Lab Eta Factory will improve existing measurements of rare η/η' decays by a few orders of magnitude, and the proposed REDTOP experiment aims to produce an unprecedented sample of $10^{14}(10^{12})$ $\eta(\eta')$ mesons. These will offer unique opportunities to probe BSM physics in the unflavored meson sector.

2 Theoretical framework

2.1 ALP- χ PT Lagrangian and leading order decay amplitudes

Generic ALP models show a diverse range of phenomenological signatures due to the many ways in which ALPs can couple to Standard Model particles. In this study, we shall concentrate on flavor-preserving ALP couplings to quarks and gluons, which control η/η' decays to final states containing hadrons and one or more ALPs. In particular, we will ignore more generic ALP interactions involving flavor-changing transitions, which are important in, e.g., Kaon and B-meson decays. We will also omit ALP couplings to photons and leptons; while they do not affect axio-hadronic η/η' decays, they are key parameters in determining the ALP's decay modes and lifetime, especially for ALP masses below the hadronic decay threshold, $m_a < 3m_{\pi}$. Generically, light ALPs produced in η/η' decays will either decay promptly to visible final states (e.g., $a \to \ell^+\ell^-$, $a \to \gamma\gamma$), or will travel a macroscopic distance before decaying, leading to events with displaced vertices or missing energy. When designing experimental ALP searches, one must combine our results for axio-hadronic η/η' decay rates with additional assumptions for the ALP decay modes and lifetime.

Several bases have been considered in the literature to express low energy ALP couplings. Here, we choose a basis in which the ALP couplings to quarks are exclusively expressed as Yukawa couplings (instead of derivative couplings). Not only this basis makes calculations more convenient, but this is often the more natural basis for UV completions of ALP models. The Lagrangian in this Yukawa basis can be written as:

$$\mathcal{L}_{\mathrm{ALP}}^{Y} \supset \frac{1}{2} \partial_{\mu} a \partial^{\mu} a - \frac{1}{2} M_{\mathcal{PQ}}^{2} a^{2} - Q_{G} \frac{\alpha_{s}}{8\pi} \frac{a}{f_{a}} G \tilde{G} + \sum_{q=u,d,s} m_{q} \bar{q} \left(e^{iQ_{q} \frac{a}{f_{a}} \gamma_{5}} \right) q. \tag{2.1}$$

Above, M_{PQ} is a bare PQ-breaking contribution to the ALP mass; f_a is the ALP decay constant; $G\tilde{G} \equiv \epsilon_{\mu\nu\alpha\beta}G_{\mu\nu}G^{\alpha\beta}$ with $G_{\mu\nu}$ denoting the gluon field strength tensor; and the PQ charges Q_G and Q_q parametrize the ALP couplings to gluons and quarks, respectively. Note that (2.1) is defined at the GeV scale with the heavy quarks c, b, t integrated out. Their PQ charges contribute implicitly to the ALP-gluon coupling through:

$$Q_G \equiv Q_G^{\text{UV}} + Q_c + Q_b + Q_t \,. \tag{2.2}$$

By performing ALP-dependent chiral rotations of the quark fields, $q \to \exp(i\gamma_5 \frac{Q_q}{2} \frac{a}{f_a})q$, we can re-express the ALP model in (2.1) in an equivalent basis in which the ALP couples only derivatively to fermions [74]:

$$\mathcal{L}_{\text{ALP}}^{\partial} \supset -\left(Q_{G}^{\text{UV}} + \sum_{q} Q_{q}\right) \frac{\alpha_{s}}{8\pi} \frac{a}{f_{a}} G \tilde{G} + \frac{\partial_{\mu} a}{f_{a}} \sum_{q=u,d,s} \frac{Q_{q}}{2} \bar{q} \gamma^{\mu} \gamma^{5} q$$

$$+ \sum_{i,j} \frac{g_{2}}{\sqrt{2}} V_{ij}^{\text{CKM}} W_{\mu}^{+} \bar{u}_{L}^{i} e^{-i\left(\frac{Q_{u_{i}} - Q_{d_{j}}}{2} \frac{a}{f_{a}} \gamma_{5}\right)} \gamma^{\mu} d_{L}^{j} + \text{h.c.}$$

$$(2.3)$$

The flavor-changing term in (2.3) comes from chirally rotating the weak currents; it is often omitted in the literature, but it is necessary for the equivalency between (2.1) and (2.3)

and for a consistent description of flavor-changing axionic meson decays [54]. Since in this study we are focused on flavor-conserving processes, this subtlety in basis-equivalency is not a concern to us. We shall now proceed with the Yukawa-basis representation of the ALP interactions in (2.1).

In order to extract the amplitudes for the decays $\eta/\eta' \to \pi\pi a$ we need a framework to describe ALP interactions with mesons. The first step is to map the QCD level Lagrangian $\mathcal{L}_{\text{ALP}}^{Y}$ in (2.1) into Chiral Perturbation Theory (χ PT) [75]. Because we care about decays of the η' meson, we carry out our study relying on Large- N_C χ PT [76–79]. We recall that the large mass of the η' meson (which is composed predominantly of the pseudoscalar singlet η_0) comes from the anomalous breaking of the U(1)_A global symmetry by the gluon density operator $G\tilde{G}$, which prevents the η_0 state to be a pseudo-Nambu-Goldstone boson (pNGB). In the $N_C \to \infty$ limit, however, the U(1)_A axial anomaly vanishes and the η_0 —absent in the standard U(3) χ PT—becomes a new light degree-of-freedom of the effective theory, i.e., the ninth pNGB associated with the spontaneous symmetry breaking of U(3)_L × U(3)_R \to U(3)_V. In this regard, we map the ALP-gluon coupling term in (2.1) into χ PT in a similar fashion as the η_0 , following the heuristic prescription in [80].

Within this framework, the leading order ALP- χ PT Lagrangian can be written as [64]:

$$\mathcal{L}_{\text{ALP}}^{\chi \text{PT@LO}} = \frac{1}{2} \partial_{\mu} a \partial^{\mu} a - \frac{1}{2} M_{\text{pq}}^{2} a^{2} - \frac{1}{2} m_{0}^{2} \left(\eta_{0} - \frac{Q_{G}}{\sqrt{6}} \frac{f_{\pi}}{f_{a}} a \right)^{2} + \frac{f_{\pi}^{2}}{4} \text{Tr} \left[\partial_{\mu} U^{\dagger} \partial^{\mu} U \right] + \frac{f_{\pi}^{2}}{4} \text{Tr} \left[2B_{0} (M_{q}(a)U + M_{q}(a)^{\dagger} U^{\dagger}) \right], \qquad (2.4)$$

where $f_{\pi} = 92.07$ MeV [2] is the pion decay constant; B_0 is a low energy constant related to the quark condensate, $\delta^{ij}B_0 = -\langle q^i\bar{q}^j\rangle/f_{\pi}^2$; m_0 parametrizes the U(1)_A anomaly contribution to the mass of the chiral singlet η_0 ; $M_q(a)$ is the ALP-dependent quark mass matrix,

$$M_q(a) \equiv \begin{pmatrix} m_u e^{iQ_u a/f_a} \\ m_d e^{iQ_d a/f_a} \\ m_s e^{iQ_s a/f_a} \end{pmatrix}, \qquad (2.5)$$

and U is the nonlinear representation of the pNGB chiral meson nonet,

$$U \equiv \exp\left(\frac{i\sqrt{2}\Phi}{f_{\pi}}\right),\tag{2.6}$$

with

$$\Phi \equiv \begin{pmatrix}
\frac{1}{\sqrt{2}}\pi_3 + \frac{1}{\sqrt{6}}\eta_8 + \frac{1}{\sqrt{3}}\eta_0 & \pi^+ & K^+ \\
\pi^- & -\frac{1}{\sqrt{2}}\pi_3 + \frac{1}{\sqrt{6}}\eta_8 + \frac{1}{\sqrt{3}}\eta_0 & K^0 \\
K^- & K^0 & -\frac{2}{\sqrt{6}}\eta_8 + \frac{1}{\sqrt{3}}\eta_0
\end{pmatrix}.$$
(2.7)

The quadratic mass term in (2.4) mixes the ALP field a with the neutral, strangeness-zero chiral mesons fields π_3 , η_8 and η_0 . We can express these quadratic Lagrangian terms

as $\mathcal{L}_{\text{ALP}}^{\chi \text{PT@LO}} \supset -\frac{1}{2}\phi^T \mathbb{M}_{\phi}^2 \phi$ with $\phi \equiv (\pi_3, \eta_8, \eta_0, a)$, and

$$\mathbf{M}_{\phi}^{2} = \begin{pmatrix} \mu_{\pi_{3}}^{2} & \mu_{\pi_{3}\eta_{8}}^{2} & \mu_{\pi_{3}\eta_{0}}^{2} & \mu_{a\pi}^{2} \\ \mu_{\eta_{8}}^{2} & \mu_{\eta_{8}\eta_{0}}^{2} & \mu_{a\eta_{8}}^{2} \\ \mu_{\eta_{0}}^{2} & \mu_{a\eta_{0}}^{2} & \mu_{a\eta_{0}}^{2} \\ \mu_{\alpha}^{2} & \mu_{\alpha}^{2} \end{pmatrix},$$
(2.8)

where

$$\mu_{\pi_3}^2 = B_0(m_u + m_d), \tag{2.9}$$

$$\mu_{\pi_3\eta_8}^2 = \frac{B_0}{\sqrt{3}}(m_u - m_d), \tag{2.10}$$

$$\mu_{\pi_3\eta_0}^2 = \sqrt{\frac{2}{3}}B_0(m_u - m_d), \tag{2.11}$$

$$\mu_{\eta_8}^2 = \frac{B_0}{3}(m_u + m_d + 4m_s), \tag{2.12}$$

$$\mu_{\eta_8\eta_0}^2 = \frac{\sqrt{2}}{3} B_0(m_u + m_d - 2m_s), \tag{2.13}$$

$$\mu_{\eta_0}^2 = m_0^2 + \frac{2}{3}B_0(m_u + m_d + m_s), \tag{2.14}$$

$$\mu_{a\pi_3}^2 = \frac{f_\pi}{f_a} B_0(m_u Q_u - m_d Q_d), \tag{2.15}$$

$$\mu_{a\eta_8}^2 = \frac{f_\pi}{f_a} \frac{B_0}{\sqrt{3}} (m_u Q_u + m_d Q_d - 2m_s Q_s), \tag{2.16}$$

$$\mu_{a\eta_0}^2 = \frac{f_{\pi}}{f_a} \sqrt{\frac{2}{3}} B_0(m_u Q_u + m_d Q_d + m_s Q_s) - \frac{f_{\pi}}{f_a} m_0^2 \frac{Q_G}{\sqrt{6}}, \tag{2.17}$$

$$\mu_a^2 = \frac{f_\pi^2}{f_a^2} B_0(m_u Q_u^2 + m_d Q_d^2 + m_s Q_s^2) + \frac{f_\pi^2}{f_a^2} m_0^2 \frac{Q_G^2}{6} + M_{\text{PQ}}^2.$$
 (2.18)

In order to obtain the physical ALP state $a_{\rm phys}$ and meson states π^0 , η and η' , the mass matrix in (2.8) needs to be diagonalized. This process can be done in two steps. The first step is the removal of the ALP-meson mixing terms, parametrized by the angles $\theta_{a\pi}$, $\theta_{a\eta_8}$, $\theta_{a\eta_0}$. The second step is the diagonalization of the chiral meson mass terms. The resulting relations between the original and physical states are:

$$\begin{pmatrix}
\pi_{3} \\
\eta_{8} \\
\eta_{0} \\
a
\end{pmatrix} = \begin{pmatrix}
1_{3\times3} & \theta_{a\eta_{8}} \\
\theta_{a\eta_{0}} \\
-\theta_{a\pi} - \theta_{a\eta_{8}} - \theta_{a\eta_{0}} & 1
\end{pmatrix}
\begin{pmatrix}
R_{3\times3} & 0 \\
0 & 0 \\
0 & 0 & 1
\end{pmatrix}
\begin{pmatrix}
\pi^{0} \\
\eta \\
\eta' \\
a_{\text{phys}}
\end{pmatrix}, (2.19)$$

where \mathbb{R} is an orthogonal matrix that diagonalizes of the π^0 - η - η' meson subsystem, given by [81, 82]:

$$\mathbb{R} = \begin{pmatrix} 1 & -\theta_{\pi\eta} & -\theta_{\pi\eta'} \\ (\theta_{\pi\eta}\cos\theta_{\eta\eta'} + \theta_{\pi\eta'}\sin\theta_{\eta\eta'}) & \cos\theta_{\eta\eta'} & \sin\theta_{\eta\eta'} \\ (\theta_{\pi\eta'}\cos\theta_{\eta\eta'} - \theta_{\pi\eta}\sin\theta_{\eta\eta'}) & -\sin\theta_{\eta\eta'}\cos\theta_{\eta\eta'} \end{pmatrix}. \tag{2.20}$$

Above, $\theta_{\eta\eta'}$, $\theta_{\pi\eta}$, and $\theta_{\pi\eta'}$ are, respectively, the η_8 - η_0 , π_3 - η_8 , and π_3 - η_0 mixing angles.

For our phenomenological analysis in Sec. 4, we will use the η - η' mixing angle measured by KLOE, and also set $\theta_{\eta\eta'} = -13.3(5)^{\circ}$ [83], $m_0 = 1.03$ GeV [84], and $\theta_{\pi\eta} = 0.018$, $\theta_{\pi\eta'} = 0.0049$ [59]. This choice results in leading order physical masses of $m_{\eta}^{(0)} = 534$ MeV for the η meson and $m_{\eta'}^{(0)} = 1.14$ GeV for the η' meson, which disagree significantly with the experimental values of $m_{\eta} = 548$ MeV and $m_{\eta'} = 958$ MeV. Resolving this discrepancy requires one to go to next-to-leading order in the χ PT expansion [85], which is beyond the scope of this work. In what follows we will adopt this numerical choice of parameters, but use the experimental values for the η and η' masses when computing their decay rates.

It is relatively straightforward to obtain the ALP-meson mixing terms $\theta_{a\pi}$, $\theta_{a\eta_8}$, $\theta_{a\eta_0}$ in $(2.19)^2$. Working first in the PQ-preserving limit $M_{\text{PQ}} = 0$ (in which case the ALP can be identified with the QCD axion), the mass-squared of the physical axion a_{phys} is given by

$$(m_a^{(PQ)})^2 = (Q_u + Q_d + Q_s + Q_G)^2 \frac{B_0 m_u m_d m_s}{\left(m_u m_d + m_u m_s + m_d m_s + \frac{6B_0 m_u m_d m_s}{m_0^2}\right)} \frac{f_\pi^2}{f_a^2}, \quad (2.21)$$

and the axion-meson mixing angles are given by

$$\theta_{a\pi}^{(PQ)} = -\frac{f_{\pi}}{f_a} \frac{1}{(1+\epsilon)} \left(\frac{Q_u m_u - Q_d m_d}{m_u + m_d} + \frac{m_u - m_d}{m_u + m_d} \frac{Q_s + Q_G}{2} + \epsilon \frac{Q_u - Q_d}{2} \right), \tag{2.22}$$

$$\theta_{a\eta_8}^{(PQ)} = \frac{f_{\pi}}{f_a} \frac{\sqrt{3}}{2} \frac{1}{(1+\epsilon)} \left(Q_s + \frac{Q_G}{3} - \epsilon \frac{(Q_u + Q_d + 2Q_G/3) + \frac{2B_0 m_s}{m_0^2} (Q_u + Q_d - 2Q_s)}{1 + \frac{6B_0 m_s}{m_0^2}} \right), (2.23)$$

$$\theta_{a\eta_0}^{(PQ)} = \frac{f_{\pi}}{f_a} \frac{1}{\sqrt{6}} \frac{1}{(1+\epsilon)} \left(Q_G + \epsilon \frac{Q_G - \frac{6B_0 m_s}{m_0^2} (Q_u + Q_d + Q_s)}{1 + \frac{6B_0 m_s}{m_0^2}} \right), \tag{2.24}$$

where the small parameter ϵ , of order $\mathcal{O}(m_{\pi}^2/m_K^2)$, is given by

$$\epsilon \equiv \frac{m_u m_d}{m_s (m_u + m_d)} \left(1 + 6 \, \frac{B_0 m_s}{m_0^2} \right) \approx 0.04.$$
(2.25)

Next, we can consider the PQ-breaking case with a finite M_{PQ} mass (when the ALP is no longer the QCD axion). Here, we assume that $f_a \gg f_{\pi}$ and neglect terms of $\mathcal{O}(\theta_{a\phi}^2)$, where $\phi = \pi_3$, η_8 , η_0 . In this case, the mass-squared of the physical ALP $a_{\rm phys}$ is:

$$m_a^2 = (m_a^{(PQ)})^2 + M_{PO}^2.$$
 (2.26)

Neglecting π - η and π - η' mixing (i.e., making the approximation of $\theta_{\pi \eta^{(\prime)}} \to 0$), the ALP-

²A simple trick is to integrate out the π_3 , η_8 and η_0 states via the equations of motion.

meson mixing angles are given by

$$\theta_{a\pi} = \theta_{a\pi}^{(PQ)} \left(1 + \frac{M_{pQ}^{2}}{m_{\pi}^{2} - m_{a}^{2}} \right), \qquad (2.27a)$$

$$\theta_{a\eta_{8}} = \theta_{a\eta_{8}}^{(PQ)} \left(1 + \cos^{2}\theta_{\eta\eta'} \frac{M_{pQ}^{2}}{m_{\eta}^{2} - m_{a}^{2}} + \sin^{2}\theta_{\eta\eta'} \frac{M_{pQ}^{2}}{m_{\eta'}^{2} - m_{a}^{2}} \right) \qquad (2.27b)$$

$$+ \theta_{a\eta_{0}}^{(PQ)} \frac{\sin 2\theta_{\eta\eta'}}{2} \left(\frac{M_{pQ}^{2}}{m_{\eta'}^{2} - m_{a}^{2}} - \frac{M_{pQ}^{2}}{m_{\eta}^{2} - m_{a}^{2}} \right), \qquad (2.27c)$$

$$\theta_{a\eta_{0}} = \theta_{a\eta_{0}}^{(PQ)} \left(1 + \sin^{2}\theta_{\eta\eta'} \frac{M_{pQ}^{2}}{m_{\eta}^{2} - m_{a}^{2}} + \cos^{2}\theta_{\eta\eta'} \frac{M_{pQ}^{2}}{m_{\eta'}^{2} - m_{a}^{2}} \right) \qquad (2.27c)$$

$$+ \theta_{a\eta_{8}}^{(PQ)} \frac{\sin 2\theta_{\eta\eta'}}{2} \left(\frac{M_{pQ}^{2}}{m_{\eta'}^{2} - m_{a}^{2}} - \frac{M_{pQ}^{2}}{m_{\eta'}^{2} - m_{a}^{2}} \right).$$

Note that the expressions above are only valid in the small mixing angle approximation, i.e., when $\theta_{a\pi}^{(\text{PQ})}$, $\theta_{a\eta_8}^{(\text{PQ})}$, $\theta_{a\eta_9}^{(\text{PQ})} \ll 1$; $M_{\text{PQ}}^2/|m_\pi^2 - m_a^2| \ll f_a/f_\pi$ for (2.27a); and $M_{\text{PQ}}^2/|m_{\eta^{(\prime)}}^2 - m_a^2| \ll f_a/f_\pi$ for (2.27b) and (2.27c).

We are now in a position to obtain the leading order amplitudes³ for $\eta^{(\prime)} \to \pi^0 \pi^0 a$, $\eta^{(\prime)} \to \pi^+ \pi^- a$, and $\eta^\prime \to \eta \pi^0 a$. These follow from the ALP Lagrangian in (2.4) with the field redefinitions from (2.19):

$$\mathcal{A}(\eta \to \pi^{0}\pi^{0}a) = \frac{m_{\pi}^{2}}{f_{\pi}^{2}} \left[C_{\eta} \frac{(m_{u}A_{u} + m_{d}A_{d})}{m_{u} + m_{d}} + \left(2\theta_{\pi\eta'}C_{\eta}C_{\eta'} + \theta_{\pi\eta}(C_{\eta}^{2} - C_{\eta'}^{2}) \right) \frac{(m_{u}A_{u} - m_{d}A_{d})}{m_{u} + m_{d}} \right],
+ \left(2\theta_{\pi\eta'}C_{\eta}C_{\eta'} + \theta_{\pi\eta}(C_{\eta'}^{2} - C_{\eta'}^{2}) \right) \frac{(m_{u}A_{u} - m_{d}A_{d})}{m_{u} + m_{d}} \right],
+ \left(2\theta_{\pi\eta}C_{\eta}C_{\eta'} + \theta_{\pi\eta'}(C_{\eta'}^{2} - C_{\eta}^{2}) \right) \frac{(m_{u}A_{u} - m_{d}A_{d})}{m_{u} + m_{d}} \right],
+ \left(2\theta_{\pi\eta}C_{\eta}C_{\eta'} + \theta_{\pi\eta'}(C_{\eta'}^{2} - C_{\eta}^{2}) \right) \frac{(m_{u}A_{u} - m_{d}A_{d})}{m_{u} + m_{d}} \right],
+ \left(2\theta_{\pi\eta}C_{\eta}C_{\eta'} + \theta_{\pi\eta'}(C_{\eta'}^{2} - C_{\eta}^{2}) \right) \frac{(m_{u}A_{u} - m_{d}A_{d})}{m_{u} + m_{d}} \right],
+ \left(2\theta_{\pi\eta}C_{\eta}C_{\eta'} + \theta_{\pi\eta'}(C_{\eta'}^{2} - C_{\eta}^{2}) \right) \frac{(m_{u}A_{u} - m_{d}A_{d})}{m_{u} + m_{d}} \right],$$

$$(2.30)$$

$$- \theta_{\pi\eta} \frac{(m_{u}A_{u} - m_{d}A_{d})}{m_{u} + m_{d}} - \theta_{\pi\eta} \frac{\theta_{a\pi}}{f_{\pi}^{2}} \left[s - \frac{m_{\eta}^{2} + 2m_{\pi}^{2} + m_{a}^{2}}{3} \right],$$

³In order to lighten the notation, we shall suppress from this point forward the subscript in the physical ALP state, i.e., we will take $a_{\text{phys}} \to a$.

$$\mathcal{A}(\eta' \to \pi^{+} \pi^{-} a) = \frac{m_{\pi}^{2}}{f_{\pi}^{2}} \left[C_{\eta'} \frac{(m_{u} A_{u} + m_{d} A_{d} - 2(m_{u} - m_{d}) \theta_{a\pi}/3)}{m_{u} + m_{d}} \right] - \theta_{\pi \eta'} \frac{(m_{u} A_{u} - m_{d} A_{d})}{m_{u} + m_{d}} - \theta_{\pi \eta'} \frac{\theta_{a\pi}}{f_{\pi}^{2}} \left[s - \frac{m_{\eta'}^{2} + 2m_{\pi}^{2} + m_{a}^{2}}{3} \right],$$

$$\mathcal{A}(\eta' \to \eta \pi^{0} a) = \frac{m_{\pi}^{2}}{f_{\pi}^{2}} \left[C_{\eta} C_{\eta'} \frac{(m_{u} A_{u} - m_{d} A_{d})}{m_{u} + m_{d}} - \theta_{\pi \eta} C_{\eta'}^{2} \frac{(m_{u} A_{u} + m_{d} A_{d}) C_{\eta'} - 4m_{s} A_{s} C_{\eta}}{m_{u} + m_{d}} - \theta_{\pi \eta'} C_{\eta}^{2} \frac{(m_{u} A_{u} + m_{d} A_{d}) C_{\eta} + 4m_{s} A_{s} C_{\eta'}}{m_{u} + m_{d}} \right],$$

$$(2.31)$$

where $m_{\pi}^2 \equiv B_0(m_u + m_d)$ is the leading order pion mass in the isospin limit; the Mandelstam variable s is defined as $s \equiv (p_{\eta} - p_a)^2$ (see Subsec. 2.2); and

$$C_{\eta} \equiv \frac{\cos\theta_{\eta\eta'}}{\sqrt{3}} - \frac{\sin\theta_{\eta\eta'}}{\sqrt{3/2}},\tag{2.33}$$

$$C_{\eta'} \equiv \frac{\cos\theta_{\eta\eta'}}{\sqrt{3/2}} + \frac{\sin\theta_{\eta\eta'}}{\sqrt{3}},\tag{2.34}$$

$$A_u \equiv \frac{f_{\pi}}{f_a} Q_u + \theta_{a\pi} + \frac{\theta_{a\eta_8}}{\sqrt{3}} + \frac{\theta_{a\eta_0}}{\sqrt{3/2}},$$
 (2.35)

$$A_d \equiv \frac{f_{\pi}}{f_a} Q_d - \theta_{a\pi} + \frac{\theta_{a\eta_8}}{\sqrt{3}} + \frac{\theta_{a\eta_0}}{\sqrt{3/2}},$$
 (2.36)

$$A_s \equiv \frac{f_{\pi}}{f_a} \frac{Q_s}{\sqrt{2}} - \frac{\theta_{a\eta_8}}{\sqrt{3/2}} + \frac{\theta_{a\eta_0}}{\sqrt{3}}.$$
 (2.37)

The amplitudes in (2.28)–(2.32) scale as $\sim 1/f_a$ and receive contributions from a direct $a\pi\pi\eta^{(\prime)}$ quartic term in the leading order Lagrangian, as well as from mixing terms stemming from quartic SM meson interactions where one meson state mixes with the ALP⁴. Note also that subleading terms involving $\pi - \eta^{(\prime)}$ mixing (i.e., proportional to $\theta_{\pi\eta^{(\prime)}}$) generally provide only percent-level corrections to the total amplitudes in (2.28)–(2.31), and in most cases can be neglected. The one instance in which the $\theta_{\pi\eta^{(\prime)}}$ -suppressed contributions are important is in the KSVZ QCD axion limit of (2.32) (i.e., with $M_{\text{PQ}} = 0$, $Q_q = 0$, and finite Q_G^{UV}). In this case, the first term in (2.32) vanishes identically (cf. (2.22), (2.23) and (2.24)), leaving the $\theta_{\pi\eta^{(\prime)}}$ -suppressed terms as the dominant leading order contributions to $\mathcal{A}(\eta' \to \eta\pi^0 a)$.

2.2 Decay kinematics

Before moving on to the main section of this paper, we briefly outline our conventions for kinematic variables. We define the amplitude for the decay $\eta \to \pi \pi a$ in the usual way,

$$\langle \pi^{i}(p_{1})\pi^{j}(p_{2})a(p_{a})|T|\eta(p_{\eta})\rangle = (2\pi)^{4}\delta^{4}(p_{\eta} - p_{1} - p_{2} - p_{a})\delta^{ij}\mathcal{M}(s, t, u), \qquad (2.38)$$

⁴See Refs. [52, 53, 64] for similar calculations of these amplitudes, and Ref. [50] for a calculation of the related amplitude $a \to \pi\pi\eta^{(\prime)}$.

where i, j refer to the isospin indices of the pion. In the following, we will consider both the neutral $\eta \to \pi^0 \pi^0 a$ and charged $\eta \to \pi^+ \pi^- a$ decay channels, which only differ by isospin-breaking effects. The Mandelstam variables for the decay process are given by:

$$s = (p_n - p_a)^2 = (p_1 + p_2)^2, (2.39)$$

$$t = (p_{\eta} - p_1)^2 = (p_2 + p_a)^2, (2.40)$$

$$u = (p_{\eta} - p_2)^2 = (p_1 + p_a)^2,$$
 (2.41)

which fulfill the relation

$$s + t + u = m_{\eta}^2 + 2m_{\pi}^2 + m_a^2. (2.42)$$

In the center-of-mass system of the two pions, t and u can be expressed in terms of s and θ_s according to

$$t(s,\cos\theta_s) = \frac{1}{2} \left(m_\eta^2 + 2m_\pi^2 + m_a^2 - s + \kappa_{\pi\pi}(s)\cos\theta_s \right), \qquad (2.43)$$

$$u(s,\cos\theta_s) = \frac{1}{2} \left(m_\eta^2 + 2m_\pi^2 + m_a^2 - s - \kappa_{\pi\pi}(s)\cos\theta_s \right), \qquad (2.44)$$

where $\cos \theta_s$ refers to the scattering angle,

$$\cos \theta_s \equiv \frac{t - u}{\kappa_{\pi\pi}(s)} \,, \quad \kappa_{\pi\pi}(s) \equiv \sigma_{\pi}(s) \lambda^{1/2}(m_{\eta}^2, m_a^2, s) \,, \tag{2.45}$$

with $\sigma_{\pi}(s) \equiv \sqrt{1 - 4m_{\pi}^2/s}$, and the Källen function $\lambda(a, b, c) \equiv a^2 + b^2 + c^2 - 2(ab + ac + bc)$. The partial decay rate is given by [2]

$$\Gamma(\eta \to \pi \pi a) = \frac{1}{S_{\pi_1 \pi_2}} \frac{1}{(2\pi)^3} \frac{1}{32m_{\eta}^3} \int ds \, dt \, |\mathcal{M}(s, t, u)|^2 \,, \tag{2.46}$$

where $S_{\pi_1\pi_2}$ is a combinatorial factor that accounts for the number of identical particles in the final state; in particular, $S_{\pi^+\pi^-} = 1$ and $S_{\pi^0\pi^0} = 2!$. The boundaries of the physical decay region in t lie within the interval $[t_{\min}(s), t_{\max}(s)]$, with

$$t_{\text{max/min}}(s) = \frac{1}{2} \left[m_{\eta}^2 + m_a^2 + 2m_{\pi}^2 - s \pm \frac{\lambda^{1/2}(s, m_{\eta}^2, m_a^2)\lambda^{1/2}(s, m_{\pi}^2, m_{\pi}^2)}{s} \right], \quad (2.47)$$

while the allowed range for s is

$$s_{\min} = 4m_{\pi}^2, \quad s_{\max} = (m_{\eta} - m_a)^2.$$
 (2.48)

The region defined by (2.47) and (2.48) defines the Dalitz phase space.

The derivation of the decay rate for the analogous reaction $\eta' \to \pi \pi a$ is formally identical to that of (2.46) with the appropriate replacements, e.g., $m_{\eta} \to m_{\eta'}$.

3 Pion-pion final state interactions with dispersion relations

In any process with hadrons in the final state, final state interactions (FSI) from strong rescattering effects must be taken into account if one aims to make predictions with a reasonable degree of accuracy.

A model independent approach that ressums FSI is given by dispersion theory. Based on the fundamental physical principles of unitarity and analyticity, dispersion relations determine the amplitude up to certain subtraction constants that can be fixed by matching to the results of the effective theory, or from fits to experimental data, when available.

Because the ressummation of the FSI is imposed by construction, it becomes specially relevant and useful where perturbative, EFT-based approaches, such as χ PT, are doomed to fail. This is generically the case of low energy hadronic processes involving low-lying QCD resonances in the physical region, such as the SM decays $\eta/\eta' \to 3\pi$ [86] and $\eta' \to \eta\pi\pi$ [87], as well as the BSM decays $\eta/\eta' \to \pi\pi a$ we wish to consider here. In particular, the final state pions in these processes undergo strong FSI that could significantly perturb the spectrum, most notably in the isospin-zero S-wave channel with the corresponding appearance of the σ meson resonance.

Alternative approaches to the treatment of FSI are unitarized versions of χ PT, such as the Inverse Amplitude Method [88–91] or the N/D method [92–94]. However, in addition to the uncertainties in the determination of the low energy constants of the $\mathcal{O}(p^4)$ χ PT Lagrangian, these methods yield amplitudes that may not satisfy exact unitarity⁵ [97–100]. We therefore opt for the dispersive method over these alternative approaches for our analysis. In the following, we present a detailed application of dispersion relations to the axio-hadronic $\eta/\eta' \to \pi\pi a$ decays.

Using basic theorems of complex analysis, dispersion relations connect the discontinuity of the amplitude along its branch cut to the function itself via an integral equation that can be solved in terms of the so-called Omnès equation, whose solution is given by the well-known $\pi\pi$ scattering phase shift extracted from the Roy equations [101]. In our analysis, we include the $\pi\pi$ FSI stemming from the direct s-channel and neglect crossed-channel contributions due to the lack of information on πa scattering; we shall return to this point below.

The decay amplitude $\mathcal{M}(s,t,u)$ in (2.38) can be decomposed as

$$\mathcal{M}(s,t,u) = \sum_{\ell=0}^{\infty} (2\ell+1) P_{\ell}(\cos\theta_s) m_{\ell}(s), \qquad (3.1)$$

where $P_{\ell}(\cos \theta_s)$ are the Legendre polynomials and $m_{\ell}(s)$ are the partial waves of angular momentum ℓ , which can be obtained from the full amplitude by inversion of (3.1)

$$m_{\ell}(s) = \frac{1}{2} \int_{-1}^{1} d(\cos \theta_s) P_{\ell}(\cos \theta_s) \mathcal{M}(s, t(s, \cos \theta_s), u(s, \cos \theta_s)). \tag{3.2}$$

⁵These violations of unitarity are generically small (see, e.q., refs. [95, 96]).

In practice, one can substitute the infinite sum of partial waves in the s-channel in (3.1) by three finite sums of one Mandelstam variable only [72, 102]. Explicitly,

$$\mathcal{M}(s,t,u) = \sum_{\ell=0}^{\ell_{\text{max}}} (2\ell+1) P_{\ell}(\cos\theta_s) M_{\ell}(s) + \sum_{\ell=0}^{\ell_{\text{max}}} (2\ell+1) P_{\ell}(\cos\theta_t) M_{\ell}(t) + \sum_{\ell=0}^{\ell_{\text{max}}} (2\ell+1) P_{\ell}(\cos\theta_u) M_{\ell}(u).$$
(3.3)

Isospin conservation in the decay $\eta^{(\prime)} \to \pi\pi a$ constrains the total isospin of the final state pairs $\pi\pi$ and πa to I=0 and I=1, respectively. Consequently, only even partial waves contribute. Given the smallness of the available phase space we truncate each sum in (3.3) at $\ell_{\text{max}}=0$, so that only the S-wave contributes and the decomposition of the amplitude becomes

$$\mathcal{M}(s,t,u) = M_0(s) + M_0(t) + M_0(u). \tag{3.4}$$

Projecting (3.4) into partial waves through (3.2) we obtain:

$$m_0(s) = M_0(s) + \hat{M}_0(s),$$
 (3.5)

where $\hat{M}_0(s)$ is the so-called inhomogeneity, which is given by:

$$\hat{M}_0(s) = \frac{1}{2} \int_{-1}^1 d(\cos \theta_s) \left[M_0(t(s, \cos \theta_s)) + M_0(u(s, \cos \theta_s)) \right]. \tag{3.6}$$

The structure of (3.5) is thus clear: the first term, $M_0(s)$, contains the right-hand cut contribution and accounts for s-channel $\pi\pi$ rescattering, while the second one, $\hat{M}_0(s)$, represents the s-channel projection of the left-hand cut contributions due to the t-and u-channels. One could model the left-hand cut contributions by the exchange of additional low-lying scalar resonances via Resonance Chiral Theory, such as the $a_0(980)$; however, these contributions would depend strongly on the coupling of $a_0(980)$ to the chiral mesons [53]. As we do not have information on πa scattering at our disposal, we simplify (3.5) by neglecting $\hat{M}_0(s)$.

To apply dispersion relations to the $M_0(s)$ function, one writes its unitarity relation as (see Fig. 1 for a diagrammatic interpretation):

$$\operatorname{disc} M_0(s) = 2iM_0(s)\sin \delta_0^0(s)e^{-i\delta_0^0(s)}, \qquad (3.7)$$

where the function $\delta_0^0(s)$ is the $\pi\pi$ S-wave scattering phase shift; below the first inelastic threshold (in this case, the $K\bar{K}$ threshold) the phase of the partial-wave equals $\delta_0^0(s)$, as required by Watson's final state interaction theorem [103, 104]. Given the discontinuity relation in (3.7), one can write an unsubtracted dispersion relation for $M_0(s)$ as:

$$M_0(s) = \frac{1}{2\pi i} \int_{4m_\pi^2}^{\infty} ds' \frac{\operatorname{disc} M_0(s')}{s' - s}, \qquad (3.8)$$

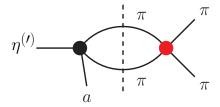


Figure 1. Schematic representation of the $\pi\pi$ contribution to the discontinuity of the partial wave $M_0(s)$ (cf. (3.7)). The black circle represents the s-channel S-wave projection of the $\eta^{(\prime)} \to \pi\pi a$ decay amplitude, while the red circle represents the S-wave $\pi\pi$ scattering amplitude.

which can be solved in terms of the usual Omnès function [105]

$$\Omega_0^0(s) = \exp\left[\frac{s}{\pi} \int_{4m_\pi^2}^{\infty} \frac{ds'}{s'} \frac{\delta_0^0(s')}{s'-s}\right].$$
(3.9)

The most general solution of (3.8) can be written as

$$M_0(s) = P(s)\Omega_0^0(s),$$
 (3.10)

where the polynomial P(s) is a real subtraction function not directly related to $\pi\pi$ rescattering. At low energies, the dispersive amplitude $M_0(s)$ can be matched to the chiral one. Performing the matching in the limit of no rescattering, i.e., $\delta_0^0(s) \to 0$, we have $\Omega_0^0(s) \to 1$, so that the subtraction polynomial P(s) in (3.10) can be identified exactly with the leading order expressions given in (2.28), (2.30), (2.29) and (2.31).

3.1 Phase shift input and Omnès function

The key input in the calculation of the Omnès equation in (3.9) is the $\pi\pi$ phase shift $\delta_0^0(s)$. For the decay $\eta \to \pi\pi a$ (as well as for $\eta' \to \pi\pi a$), the invariant mass of the pion-pion system is well below the first inelastic threshold, namely, the $K\bar{K}$ threshold. Therefore, the single-channel dispersion relation correctly describes the final state interactions, with no need to consider multichannel rescattering effects explicitly, such as those from $K\bar{K}$ intermediate states. For our analysis, we employ the parametrization for $\delta_0^0(s)$ resulting from the solution to the Roy equations [106], further imposing the asymptotic condition of $\delta_0^0(s) \to \pi$ when $s \to \infty$; this condition is reasonable since it is roughly satisfied at the $K\bar{K}$ threshold. Note that this asymptotic behavior of the phase shift implies that the Omnès function $\Omega_0^0(s)$ falls off as 1/s, as expected. Given our elastic approximation, we take $\delta_0^0(s)$ to be constant (or nearly constant) in the inelastic region above the $K\bar{K}$ threshold. This can be implemented by smoothly guiding the phase to π above $\Lambda^2 = 4m_K^2$ through [107]

$$\delta_0^0(s \ge \Lambda^2) = \pi + \left(\delta_0^0(\Lambda^2) - \pi\right) f\left(\frac{s}{\Lambda^2}\right), \quad f(x) = \frac{2}{1 + x^{3/2}}.$$
 (3.11)

Fig. 2 shows our phase shift input assuming (3.11), labelled as the central solution (solid curve). We have checked that different choices for continuation prescriptions, *e.g.*, following refs. [108, 109], result in nearly the same amplitude behavior at low energies, especially in the decay region for the processes studied here. The behavior of the partial wave in

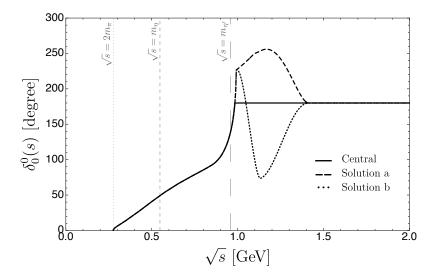


Figure 2. The three examples of phase shift inputs discussed in the text. The vertical lines indicate the phase space boundaries for the decays $\eta \to \pi\pi a$ $(2m_{\pi} \le \sqrt{s} \le m_{\eta'})$ and $\eta' \to \pi\pi a$ $(2m_{\pi} \le \sqrt{s} \le m_{\eta'})$, assuming a massless ALP.

the vicinity of the $K\bar{K}$ threshold, however, is rather ambiguous and raises the question: is the partial wave expected to have a peak or a dip around $K\bar{K}$? As this question is not easy to answer⁶, we will quantify uncertainties around and above the inelastic threshold by considering two different scenarios depending on how the partial wave of the system couples to $K\bar{K}$. On the one hand, the partial wave is expected to have a sharp peak around the position of the $f_0(980)$ if it couples strongly to $K\bar{K}$, in which case the phase shift is increased by about π while passing through the resonance. This scenario is realized in the $\pi\pi$ scattering phase shift [106], as well as in the strange scalar form factor of the pion [111, 112], and this feature is captured by solution a (dashed curve) in Fig. 2. On the other hand, a dip in the partial wave is expected if the system couples weakly to strangeness, in which case the phase quickly drops by about π with respect to the elastic approximation. This scenario is realized in the non-strange scalar form factor of the pion [111, 112], and this behavior is captured by solution b (dotted curve) in Fig. 2.

Solutions a and b for the $\pi\pi$ phase shifts in Fig. 2 follow the smoothly interpolating functions devised in Ref. [113]:

$$\delta_0^0(s)\big|_{\text{Solution a}} = \left(1 - f_{\text{int}}(s_1, s_2, s)\right) \delta_0^0(s)\big|_{(3,11)} + f_{\text{int}}(s_1, s_2, s)\pi, \tag{3.12}$$

$$\delta_0^0(s)|_{\text{Solution b}} = (1 - f_{\text{int}}(s_1, s_2, s)) \left(\delta_0^0(s)|_{(3.11)} - f_{\text{int}}(\tilde{s}_1, \tilde{s}_2, s)\pi \right) + f_{\text{int}}(s_1, s_2, s)\pi,$$
(3.13)

where

$$f_{\text{int}}(s_1, s_2, s) = \begin{cases} 0 & \text{if } s < s_1, \\ \frac{(s-s_1)^2(3s_2 - 2s - s_1)}{(s_2 - s_1)^3} & \text{if } s_1 \le s < s_2, \\ 1 & \text{if } s \ge s_2. \end{cases}$$
(3.14)

⁶One could attempt to answer this question with a full $\pi\pi$ and $K\bar{K}$ coupled-channel analysis, in the spirit of Ref. [110] for $\eta \to 3\pi$. This, however, lies beyond the scope of this work.

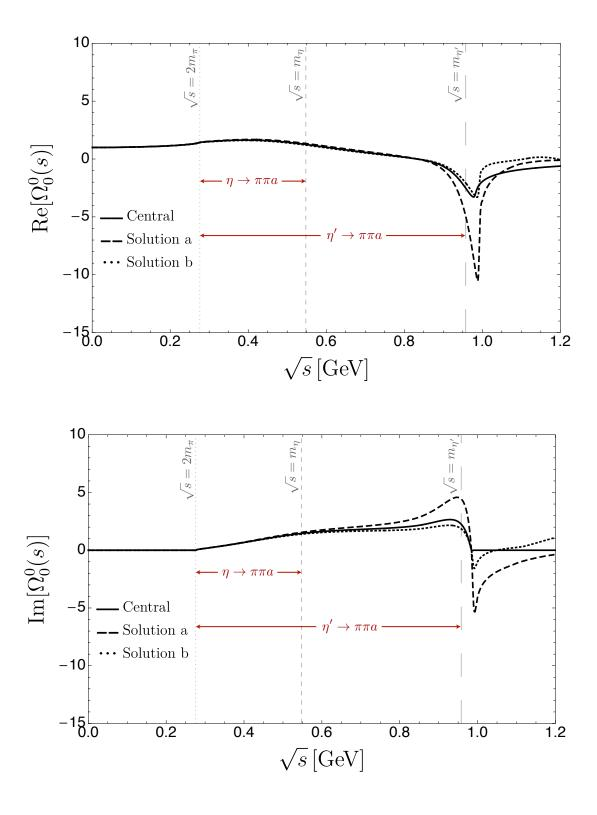


Figure 3. Real (top) and imaginary (bottom) parts of the S-wave Omnès functions (3.9) using the three phase shift examples of Fig. 2 as inputs. The red arrows indicate the phase space for the decays $\eta^{(\prime)} \to \pi\pi a$ assuming a massless ALP.

In particular, for Fig. 2 we assume $s_1 = 68m_{\pi}^2$, $s_2 = 105m_{\pi}^2$, $\tilde{s}_1 = 4m_K^2$, and $\tilde{s}_2 = \tilde{s}_1 + 16m_{\pi}^2$, although these values could be varied slightly without any significant consequence.

In Fig. 3 we show the output for the real and imaginary parts of the S-wave Omnès function (3.9) using the phase shifts of Fig. 2 as inputs. Note that the differences between the three Omnès functions are negligible in the $\eta \to \pi\pi a$ decay region (i.e., for $\sqrt{s} \le m_{\eta}$), but become non-negligible near the phase space edge of $\eta' \to \pi\pi a$ (i.e., near $\sqrt{s} = m_{\eta'}$).

Finally, for the $\eta' \to \eta \pi^0 a$ channel, we account for the $\eta \pi^0$ final state interactions following a treatment analogous to the $\pi\pi$ case described above. Specifically, following (3.10), we multiply the leading order amplitude $\mathcal{A}(\eta' \to \eta \pi^0 a)$ given in (2.32) by the isospin I=0 $\eta \pi^0$ S-wave Omnès function $\Omega_0^1(s)$ (cf. (3.9)). To obtain the $\eta \pi^0$ phase shift $\delta_0^1(s)$, and consequently $\Omega_0^1(s)$, we take the output S-wave phase for $\eta \pi^0 \to \eta \pi^0$ scattering obtained in [96], which uses a unitarized large- N_c χ PT treatment to study the decay $\eta' \to \eta \pi^0 \pi^0$.

4 Branching ratios for single ALP channels

With our results for the leading order amplitudes and the FSI corrections obtained in Secs. 2 and 3, respectively, we can now easily extract the branching ratios for the single ALP decays $\eta^{(\prime)} \to \pi\pi a$ and $\eta' \to \eta\pi a$.

For concreteness, we shall adopt two benchmark scenarios for the effective hadronic ALP couplings that have been commonly considered in the literature:

Gluon-dominance scenario

This scenario can be loosely thought of as a generalized version of the KSVZ axion [114, 115] for ALPs: the PQ symmetry acts upon some BSM sector carrying SU(3) charges that lives above the EW scale. The SM quarks are uncharged under the PQ symmetry, i.e.,

$$Q_q = 0 \text{ for } q = u, d, s, c, b, t.$$
 (4.1)

Once the PQ symmetry is explicitly and spontaneously broken and the heavy states are integrated out, both a PQ-breaking ALP mass term and an ALP-gluon coupling are generated,

$$\mathcal{L}_{\text{ALP}}^{Y} \supset -\frac{1}{2}M_{\text{PQ}}^{2}a^{2} - Q_{G}\frac{\alpha_{s}}{8\pi}\frac{a}{f_{a}}G\tilde{G},$$
 (4.2)

with

$$Q_G = Q_G^{\text{UV}} \equiv Q. \tag{4.3}$$

Quark-dominance scenario

This scenario more closely resembles a generalized version of the DFSZ axion [116, 117] for ALPs, in which all SM quarks carry flavor-universal PQ charges, and there are no additional contributions to the ALP gluon coupling from UV physics (i.e., $Q_G^{\rm UV}=0$), such that

$$Q_q \equiv Q \text{ for } q = u, d, s, c, b, t,$$
 (4.4a)

$$Q_G = Q_c + Q_b + Q_t = 3Q. (4.4b)$$

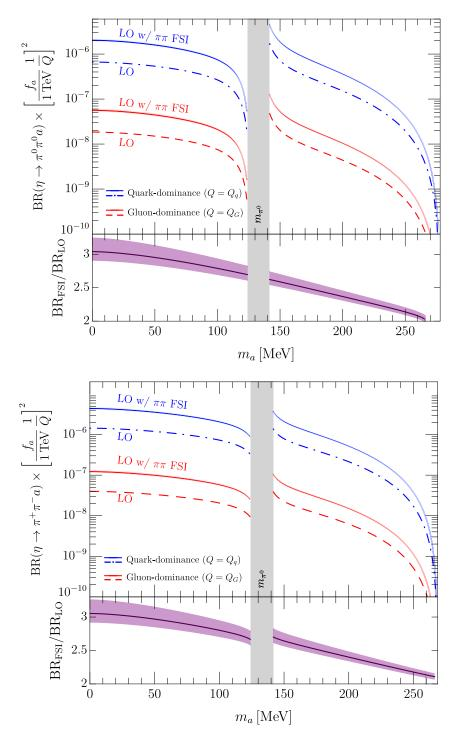


Figure 4. Branching ratios for $\eta \to \pi^0 \pi^0 a$ (top plot) and $\eta \to \pi^+ \pi^- a$ (bottom plot), as a function of the ALP mass m_a , for the quark-dominance (solid blue curve) and gluon-dominance (solid red curve) scenarios, including corrections from $\pi\pi$ final state interactions (FSI). For comparison, the corresponding leading order (LO) predictions are indicated by the (dot-)dashed curves. The bottom panels indicate the overall enhancement of the branching ratios stemming from FSI corrections relative to the LO predictions. The curves' error bands reflect the uncertainties associated with the $\pi\pi$ rescattering phase shift $\delta_0^0(s)$ (see Subsec. 3.1). Since our small mixing approximations are not valid when $m_a \approx m_{\pi^0}$ (see Subsec. 2.1), this region is masked out in the plots.

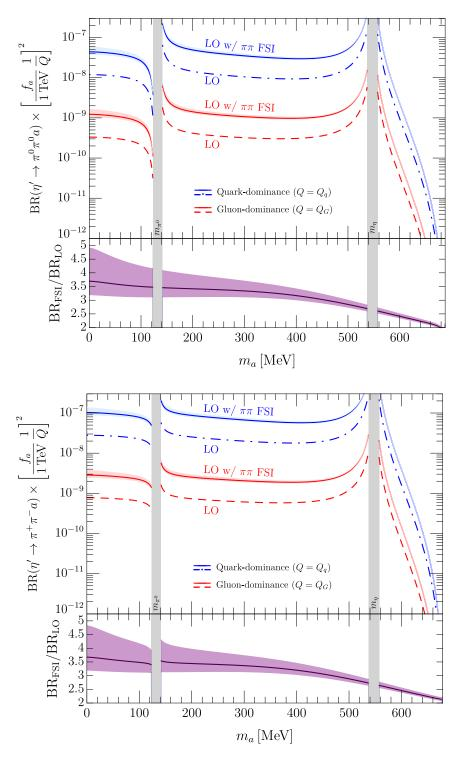


Figure 5. Branching ratios for $\eta' \to \pi^0 \pi^0 a$ (top plot) and $\eta' \to \pi^+ \pi^- a$ (bottom plot), as a function of the ALP mass m_a , for the quark-dominance (solid blue curve) and gluon-dominance (solid red curve) scenarios, including corrections from $\pi\pi$ final state interactions (FSI). For comparison, the corresponding leading order (LO) predictions are indicated by the (dot-)dashed curves. The bottom panels indicate the overall enhancement of the branching ratios stemming from FSI corrections relative to the LO predictions. The curves' error bands reflect the uncertainties associated with the $\pi\pi$ rescattering phase shift $\delta_0^0(s)$ (see Subsec. 3.1). Since our small mixing approximations are not valid when $m_a \approx m_{\pi^0}$ and $m_a \approx m_{\eta}$ (see Subsec. 2.1), these regions are masked out in the plots.

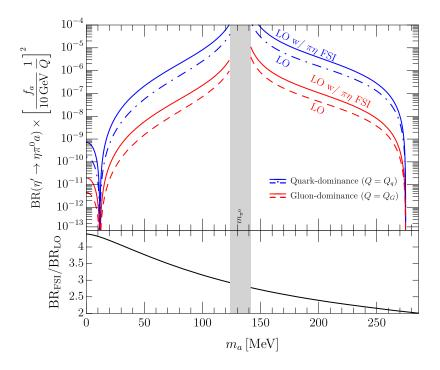


Figure 6. Branching ratio for $\eta' \to \eta \pi^0 a$, as a function of the ALP mass m_a , for the quark-dominance (solid blue curve) and gluon-dominance (solid red curve) scenarios, including corrections from $\eta \pi^0$ final state interactions (FSI). For comparison, the corresponding leading order (LO) predictions are indicated by the dashed curves. The bottom panel indicates the overall enhancement of the branching ratio stemming from FSI corrections relative to the LO prediction. Since our small mixing approximations are not valid when $m_a \approx m_{\pi^0}$, this region is masked out in the plot.

In Figs. 4, 5, and 6, we show the branching ratios for the decays $\eta^{(\prime)} \to \pi^0 \pi^0 a$, $\eta^{(\prime)} \to \pi^+ \pi^- a$, and $\eta' \to \eta \pi^0 a$ as a function of the ALP mass m_a for both the quark-dominance and gluon-dominance benchmark scenarios. The corrections due to pion-pion final state interactions are shown at the bottom panel of these figures: the curves indicate the overall enhancement of the branching ratio relative to the leading order estimate as a function of the ALP mass m_a . The error bands indicate the uncertainties associated with the $\pi\pi$ rescattering phase shift $\delta_0^0(s)$ (cf. Figs. 2 and 3). As seen, the strong rescattering effects enhance these axionic decay rates by factors ranging from $\sim 2-3$ over the kinematically allowed ALP mass range for η decays, and by factors of $\sim 2-4$ for η' decays. This clearly supports our initial argument that ALP studies based on leading order treatments, commonly seen in the literature, fall short of correctly capturing the phenomenology of hadronic ALPs, and more rigorous treatments including strong interaction effects are sorely needed.

5 Multi-ALP final states

In addition to the single ALP processes just considered, it is also worth exploring $\eta^{(\prime)}$ decay channels with multiple ALPs in the final state. Generically, the rate for emission

of n_a ALPs is suppressed by a factor of $(1/f_a)^{2n_a}$, where f_a is the ALP decay constant. Hence, for models with high scale PQ symmetry breaking, and hence with high f_a , multi-ALP channels are hopelessly outside the reach of rare $\eta^{(\prime)}$ decay searches. However, in models with f_a below the EW scale, the branching ratios for multi-ALP channels might be experimentally accessible, and in fact even competitive with single ALP channels due to much more suppressed backgrounds. While viable ALP models with $f_a < v_{\text{EW}}$ are difficult to model-build, examples exist in the literature ([13, 53, 118]).

It is straightforward to obtain the leading order amplitudes for double- and triple-ALP decay channels, such as $\eta^{(\prime)} \to \pi^0 aa$, $\eta^{\prime} \to \eta aa$, and $\eta^{(\prime)} \to aaa$. Using (2.19) and expanding the Lagrangian (2.4) in the physical ALP field to the appropriate order, we find:

$$\mathcal{A}(\eta \to \pi a a) = \frac{m_{\pi}^2}{f_{\pi}^2} C_{\eta} \frac{(m_u A_u^2 - m_d A_d^2)}{m_u + m_d}, \tag{5.1}$$

$$\mathcal{A}(\eta' \to \pi a a) = \frac{m_{\pi}^2}{f_{\pi}^2} C_{\eta'} \frac{(m_u A_u^2 - m_d A_d^2)}{m_u + m_d}, \tag{5.2}$$

$$\mathcal{A}(\eta' \to \eta a a) = \frac{m_{\pi}^2}{f_{\pi}^2} C_{\eta'} C_{\eta} \frac{(m_u A_u^2 + m_d A_d^2 - 4m_s A_s^2)}{m_u + m_d},$$

$$\mathcal{A}(\eta \to a a a) = \frac{m_{\pi}^2}{f_{\pi}^2} \frac{C_{\eta'} (m_u A_u^3 + m_d A_d^3) - 4C_{\eta'} m_s A_s^3}{m_u + m_d},$$

$$\mathcal{A}(\eta' \to a a a) = \frac{m_{\pi}^2}{f_{\pi}^2} \frac{C_{\eta'} (m_u A_u^3 + m_d A_d^3) + 4C_{\eta} m_s A_s^3}{m_u + m_d}.$$
(5.3)

$$\mathcal{A}(\eta \to aaa) = \frac{m_{\pi}^2}{f_{\pi}^2} \frac{C_{\eta}(m_u A_u^3 + m_d A_d^3) - 4C_{\eta'} m_s A_s^3}{m_u + m_d},$$
 (5.4)

$$\mathcal{A}(\eta' \to aaa) = \frac{m_{\pi}^2}{f_{\pi}^2} \frac{C_{\eta'}(m_u A_u^3 + m_d A_d^3) + 4C_{\eta} m_s A_s^3}{m_u + m_d}.$$
 (5.5)

In (5.1)-(5.5) above we have omitted the small contributions proportional to $\theta_{\pi\eta^{(\prime)}}$, and the variables C_{η} , $C_{\eta'}$, and $A_{q=u,d,s}$ have been defined in (2.33)–(2.37). Note that because the ALP-meson mixing angles, as well as the variables $A_{q=u,d,s}$, scale as $1/f_a$, the parametric dependence of the $\eta^{(\prime)}$ decay amplitudes on the ALP decay constant scales as $(1/f_a)^{n_a}$, where n_a is the number of ALPs in the final state.

In Fig. 7, we show the branching ratios for the double-ALP decay channels $\eta^{(\prime)} \to \pi^0 aa$ and $\eta' \to \eta aa$, as a function of the ALP mass m_a , for both the quark-dominance and gluon-dominance benchmark scenarios. Note that in these plots we have normalized the branching ratios to a low decay constant of $f_a = 10$ GeV, in order to display decay rates that are potentially accessible to experiments in current and future η/η' factories. We show analogous plots in Fig. 8 for the triple-ALP decay channels $\eta^{(\prime)} \to aaa$, this time normalized to an even lower decay constant of $f_a = 1$ GeV.

As with the single ALP processes, we expect that these leading order predictions will receive sizable unitarity corrections from $\pi\pi$ intermediate states. Fig. 9 illustrates a few processes that can enhance double- and triple-ALP decay channels. In particular, diagrams (a) and (b) illustrate, respectively, the contributions of $\pi\pi \to \pi a$ and $\pi\pi \to aa$ rescattering to the double-ALP channel $\eta^{(\prime)} \to \pi^0 aa$. Even neglecting complications from 3π rescattering, our results from the analysis in Sec. 3 indicate that $\pi\pi$ rescattering in the s-channel alone should provide a rate enhancement over the leading order expectation by at least a factor of 2. Similarly, diagram (c) illustrates the contribution of $\pi\pi \to aa$ rescattering to the triple-ALP channel $\eta^{(\prime)} \to aaa$, from which we expect an enhancement

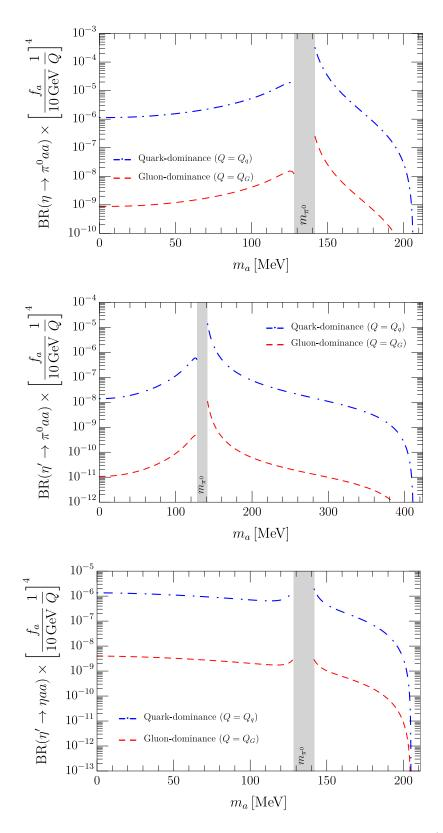


Figure 7. Leading order branching ratios for the double-ALP channels $\eta \to \pi^0 aa$ (top plot), $\eta' \to \pi^0 aa$ (middle plot), and $\eta' \to \eta aa$ (bottom plot), as a function of the ALP mass m_a , for the quark-dominance (dot-dashed blue curve) and gluon-dominance (dashed red curve) scenarios. Since our small mixing approximations are not valid when $m_a \approx m_{\pi^0}$ (see Subsec. 2.1), this region is masked out in the plots.

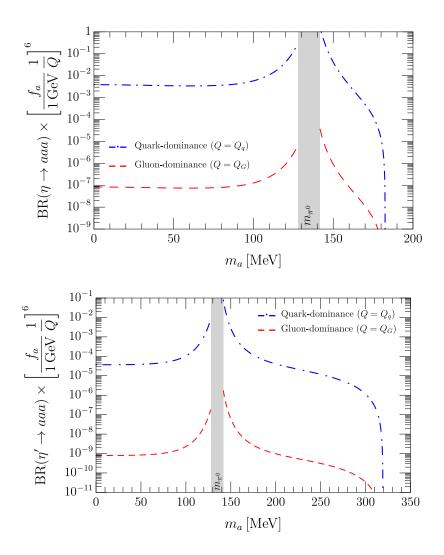


Figure 8. Leading order branching ratios for the triple-ALP channels $\eta \to aaa$ (top plot) and $\eta' \to aaa$ (bottom plot), as a function of the ALP mass m_a , for the quark-dominance (dot-dashed blue curve) and gluon-dominance (dashed red curve) scenarios. Since our small mixing approximations are not valid when $m_a \approx m_{\pi^0}$ (see Subsec. 2.1), this region is masked out in the plots.

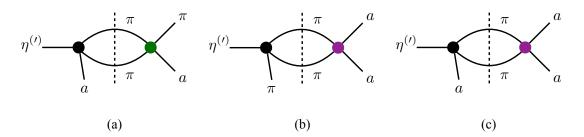


Figure 9. Schematic representation of the $\pi\pi$ rescattering contributions to the double-ALP channel $\eta^{(\prime)} \to \pi^0 aa$ (diagrams (a) and (b)), and the triple-ALP channel $\eta^{(\prime)} \to aaa$ (diagram (c)).

of the decay rates by a factor of $\sim 2.5-3$. A complete analysis of FSI corrections to multi-ALP channels in η , η' , and other meson decays is deferred to a future publication.

6 Conclusions and Outlook

In this work, we have performed a theoretical analysis of axio-hadronic decays of the η and η' mesons, paying particular attention to single ALP emission in $\eta^{(\prime)} \to \pi\pi a$ decays, where $\pi\pi = \pi^0\pi^0, \pi^+\pi^-$. Using the framework of U(3) chiral perturbation theory, we have calculated the leading order amplitudes for these processes, and using dispersion relations, we have accounted for the strong $\pi\pi$ final state interactions in a model-independent way, a significant improvement with respect to existing literature. The results of our calculations of the branching ratios as a function of the ALP mass are given in Figs. 4 and 5. We have shown that $\pi\pi$ rescattering is important in order not to underestimate these branching ratios. In particular, this effect enhances the decay rates by factors that can be as large as 3 for axio-hadronic η decays and as large as 4 for axio-hadronic η' decays. The inclusion of final state rescattering effects is the main result of this work; further improvements to include additional next-to-leading order contributions could refine the predictions presented here. We leave this investigation for future work.

We have also provided, for the first time, leading order predictions for double- and triple-ALP emission in η and η' decays, including $\eta^{(\prime)} \to \pi^0 aa$, $\eta' \to \eta aa$ and $\eta^{(\prime)} \to aaa$ (see Figs. 7 and 8). These channels can be explored in experimental searches to probe low scale PQ symmetry breaking scenarios, for which the ALP decay constant lies below the electroweak scale.

With upcoming η/η' factories in the horizon, dedicated searches for hadronic ALPs would open a new window into the exploration of strong CP solutions and low scale dark sectors. The JLab Eta Factory [63, 119], the REDTOP experiment [64], and the super τ -charm facility [120] will determine rare η and η' decays with precision several orders of magnitude higher than present measurements, and the HADES experiment at GSI plans to perform a dedicated search for $\eta \to \pi^+\pi^-(a \to e^+e^-)$ [121, 122]. Also, dedicated searches at BESIII, KLOE, and the CMS B-parking and data scouting datasets [123, 124] could probe a variety of unexplored η and η' BSM decay channels.

Our results provide a first step into improving the accuracy of predictions for axiohadronic $\eta^{(\prime)}$ decay rates by including the leading effects of non-perturbative strong dynamics through dispersion relations. In order to fully map out the space of experimental signatures, our results should be combined with further assumptions about the ALP couplings to leptons and gauge bosons to obtain their decay modes and lifetimes (see also [64]). This is particularly relevant for models of low scale ALP decay constants $f_a \lesssim \mathcal{O}(10-100)\text{TeV}$, for which the ALP can decay into visible final states—such as $\gamma\gamma$, $\ell^+\ell^-$, $\pi\pi\pi$ —with reasonably short lifetimes, yielding prompt or displaced vertices in the detector. Comprehensive phenomenological studies of all possible decay signatures to inform experimental searches are deferred to future work.

Acknowledgments

This work was supported by the DOE Office of Science High Energy Physics under contract number DE-AC52-06NA25396, and by the Laboratory Directed Research and Development program of Los Alamos National Laboratory under project number 20210944PRD2. Los Alamos National Laboratory is operated by Triad National Security, LLC, for the National Nuclear Security Administration of the U.S. Department of Energy under contract number 89233218CNA000001. DSMA acknowledges the Aspen Center for Physics (ACP) where this work was partially developed—the ACP is supported by the National Science Foundation under grant PHY-1607611. SGS is a Serra Húnter Fellow.

References

- [1] C. Hagmann, H. Murayama, G.G. Raffelt, L.J. Rosenberg and K.v. Bibber, "Axions," in Review of Particle Physics, Physics Letters B 667 (2008) 459.
- [2] Particle Data Group collaboration, Review of Particle Physics, PTEP 2022 (2022) 083C01.
- [3] J.E. Kim, Light Pseudoscalars, Particle Physics and Cosmology, Phys. Rept. 150 (1987) 1.
- [4] H.-Y. Cheng, The Strong CP Problem Revisited, Phys. Rept. 158 (1988) 1.
- [5] J.E. Kim and G. Carosi, Axions and the Strong CP Problem, Rev. Mod. Phys. 82 (2010) 557 [0807.3125].
- [6] D.J.E. Marsh, Axion Cosmology, Phys. Rept. **643** (2016) 1 [1510.07633].
- [7] D. Cadamuro and J. Redondo, Cosmological bounds on pseudo Nambu-Goldstone bosons, JCAP 02 (2012) 032 [1110.2895].
- [8] M. Millea, L. Knox and B. Fields, New Bounds for Axions and Axion-Like Particles with keV-GeV Masses, Phys. Rev. D 92 (2015) 023010 [1501.04097].
- [9] S. Hoof and J. Jaeckel, QCD axions and axionlike particles in a two-inflation scenario, Phys. Rev. D 96 (2017) 115016 [1709.01090].
- [10] P.F. Depta, M. Hufnagel and K. Schmidt-Hoberg, Robust cosmological constraints on axion-like particles, JCAP 05 (2020) 009 [2002.08370].
- [11] E. Izaguirre, T. Lin and B. Shuve, Searching for Axionlike Particles in Flavor-Changing Neutral Current Processes, Phys. Rev. Lett. 118 (2017) 111802 [1611.09355].
- [12] K. Choi, S.H. Im, C.B. Park and S. Yun, Minimal Flavor Violation with Axion-like Particles, JHEP 11 (2017) 070 [1708.00021].
- [13] D.S.M. Alves and N. Weiner, A viable QCD axion in the MeV mass range, JHEP **07** (2018) 092 [1710.03764].
- [14] L. Merlo, F. Pobbe, S. Rigolin and O. Sumensari, Revisiting the production of ALPs at B-factories, JHEP 06 (2019) 091 [1905.03259].
- [15] M. Bauer, M. Neubert, S. Renner, M. Schnubel and A. Thamm, Axionlike Particles, Lepton-Flavor Violation, and a New Explanation of a_{μ} and a_{e} , Phys. Rev. Lett. 124 (2020) 211803 [1908.00008].

- [16] C. Cornella, P. Paradisi and O. Sumensari, Hunting for ALPs with Lepton Flavor Violation, JHEP 01 (2020) 158 [1911.06279].
- [17] J. Martin Camalich, M. Pospelov, P.N.H. Vuong, R. Ziegler and J. Zupan, Quark Flavor Phenomenology of the QCD Axion, Phys. Rev. D 102 (2020) 015023 [2002.04623].
- [18] M. Bauer, M. Neubert, S. Renner, M. Schnubel and A. Thamm, Flavor probes of axion-like particles, JHEP 09 (2022) 056 [2110.10698].
- [19] T. Bandyopadhyay, S. Ghosh and T.S. Roy, ALP-Pions generalized, Phys. Rev. D 105 (2022) 115039 [2112.13147].
- [20] M. Hostert and M. Pospelov, Novel multilepton signatures of dark sectors in light meson decays, Phys. Rev. D 105 (2022) 015017 [2012.02142].
- [21] P. Agrawal et al., Feebly-interacting particles: FIPs 2020 workshop report, Eur. Phys. J. C
 81 (2021) 1015 [2102.12143].
- [22] C. Antel et al., Feebly Interacting Particles: FIPs 2022 workshop report, in Workshop on Feebly-Interacting Particles, 5, 2023 [2305.01715].
- [23] E. Armengaud et al., Conceptual Design of the International Axion Observatory (IAXO), JINST 9 (2014) T05002 [1401.3233].
- [24] S. Alekhin et al., A facility to Search for Hidden Particles at the CERN SPS: the SHiP physics case, Rept. Prog. Phys. 79 (2016) 124201 [1504.04855].
- [25] M.J. Dolan, T. Ferber, C. Hearty, F. Kahlhoefer and K. Schmidt-Hoberg, Revised constraints and Belle II sensitivity for visible and invisible axion-like particles, JHEP 12 (2017) 094 [Erratum: JHEP 03, 190 (2021)] [1709.00009].
- [26] FASER collaboration, FASER's physics reach for long-lived particles, Phys. Rev. D 99 (2019) 095011 [1811.12522].
- [27] D. Curtin et al., Long-Lived Particles at the Energy Frontier: The MATHUSLA Physics Case, Rept. Prog. Phys. 82 (2019) 116201 [1806.07396].
- [28] B. Döbrich, J. Jaeckel and T. Spadaro, Light in the beam dump ALP production from decay photons in proton beam-dumps, JHEP 05 (2019) 213 [Erratum: JHEP 10, 046 (2020)] [1904.02091].
- [29] J. Beacham et al., Physics Beyond Colliders at CERN: Beyond the Standard Model Working Group Report, J. Phys. G 47 (2020) 010501 [1901.09966].
- [30] R.R. Dusaev, D.V. Kirpichnikov and M.M. Kirsanov, Photoproduction of axionlike particles in the NA64 experiment, Phys. Rev. D 102 (2020) 055018 [2004.04469].
- [31] K.J. Kelly, S. Kumar and Z. Liu, Heavy axion opportunities at the DUNE near detector, Phys. Rev. D 103 (2021) 095002 [2011.05995].
- [32] Z. Bai et al., New physics searches with an optical dump at LUXE, Phys. Rev. D 106 (2022) 115034 [2107.13554].
- [33] A. Apyan et al., DarkQuest: A dark sector upgrade to SpinQuest at the 120 GeV Fermilab Main Injector, in Snowmass 2021, 3, 2022 [2203.08322].
- [34] J. Jaeckel, M. Jankowiak and M. Spannowsky, LHC probes the hidden sector, Phys. Dark Univ. 2 (2013) 111 [1212.3620].
- [35] K. Mimasu and V. Sanz, ALPs at Colliders, JHEP 06 (2015) 173 [1409.4792].

- [36] J. Jaeckel and M. Spannowsky, Probing MeV to 90 GeV axion-like particles with LEP and LHC, Phys. Lett. B 753 (2016) 482 [1509.00476].
- [37] S. Knapen, T. Lin, H.K. Lou and T. Melia, Searching for Axionlike Particles with Ultraperipheral Heavy-Ion Collisions, Phys. Rev. Lett. 118 (2017) 171801 [1607.06083].
- [38] I. Brivio, M.B. Gavela, L. Merlo, K. Mimasu, J.M. No, R. del Rey et al., *ALPs Effective Field Theory and Collider Signatures*, *Eur. Phys. J. C* 77 (2017) 572 [1701.05379].
- [39] M. Bauer, M. Neubert and A. Thamm, Collider Probes of Axion-Like Particles, JHEP 12 (2017) 044 [1708.00443].
- [40] M. Bauer, M. Heiles, M. Neubert and A. Thamm, Axion-Like Particles at Future Colliders, Eur. Phys. J. C 79 (2019) 74 [1808.10323].
- [41] M.B. Gavela, J.M. No, V. Sanz and J.F. de Trocóniz, Nonresonant Searches for Axionlike Particles at the LHC, Phys. Rev. Lett. 124 (2020) 051802 [1905.12953].
- [42] G.G. Raffelt, Astrophysical axion bounds, Lect. Notes Phys. 741 (2008) 51 [hep-ph/0611350].
- [43] A. Payez, C. Evoli, T. Fischer, M. Giannotti, A. Mirizzi and A. Ringwald, Revisiting the SN1987A gamma-ray limit on ultralight axion-like particles, JCAP 02 (2015) 006 [1410.3747].
- [44] J. Jaeckel, P.C. Malta and J. Redondo, Decay photons from the axionlike particles burst of type II supernovae, Phys. Rev. D 98 (2018) 055032 [1702.02964].
- [45] J.H. Chang, R. Essig and S.D. McDermott, Supernova 1987A Constraints on Sub-GeV Dark Sectors, Millicharged Particles, the QCD Axion, and an Axion-like Particle, JHEP 09 (2018) 051 [1803.00993].
- [46] R.D. Peccei and H.R. Quinn, CP Conservation in the Presence of Instantons, Phys. Rev. Lett. 38 (1977) 1440.
- [47] R.D. Peccei and H.R. Quinn, Constraints Imposed by CP Conservation in the Presence of Instantons, Phys. Rev. D 16 (1977) 1791.
- [48] S. Weinberg, A New Light Boson?, Phys. Rev. Lett. 40 (1978) 223.
- [49] F. Wilczek, Problem of Strong P and T Invariance in the Presence of Instantons, Phys. Rev. Lett. 40 (1978) 279.
- [50] D. Aloni, Y. Soreq and M. Williams, Coupling QCD-Scale Axionlike Particles to Gluons, Phys. Rev. Lett. 123 (2019) 031803 [1811.03474].
- [51] M. Bauer, M. Neubert, S. Renner, M. Schnubel and A. Thamm, *The Low-Energy Effective Theory of Axions and ALPs*, *JHEP* **04** (2021) 063 [2012.12272].
- [52] L. Gan, B. Kubis, E. Passemar and S. Tulin, Precision tests of fundamental physics with η and η' mesons, Phys. Rept. 945 (2022) 1 [2007.00664].
- [53] D.S.M. Alves, Signals of the QCD axion with mass of 17 MeV/c²: Nuclear transitions and light meson decays, Phys. Rev. D 103 (2021) 055018 [2009.05578].
- [54] M. Bauer, M. Neubert, S. Renner, M. Schnubel and A. Thamm, Consistent Treatment of Axions in the Weak Chiral Lagrangian, Phys. Rev. Lett. 127 (2021) 081803 [2102.13112].
- [55] F. Ertas and F. Kahlhoefer, On the interplay between astrophysical and laboratory probes of MeV-scale axion-like particles, JHEP 07 (2020) 050 [2004.01193].

- [56] N. Blinov, E. Kowalczyk and M. Wynne, Axion-like particle searches at DarkQuest, JHEP 02 (2022) 036 [2112.09814].
- [57] J. Jerhot, B. Döbrich, F. Ertas, F. Kahlhoefer and T. Spadaro, ALPINIST: Axion-Like Particles In Numerous Interactions Simulated and Tabulated, JHEP 07 (2022) 094 [2201.05170].
- [58] L. Di Luzio and G. Piazza, $a \to \pi\pi\pi$ decay at next-to-leading order in chiral perturbation theory, JHEP 12 (2022) 041 [Erratum: JHEP 05, 018 (2023)] [2206.04061].
- [59] R. Gao, Z.-H. Guo, J.A. Oller and H.-Q. Zhou, Axion-meson mixing in light of recent lattice η-η' simulations and their two-photon couplings within U(3) chiral theory, JHEP 04 (2023) 022 [2211.02867].
- [60] C. Cornella, A.M. Galda, M. Neubert and D. Wyler, $K^- \to \pi^- a$ at Next-to-Leading Order in Chiral Perturbation Theory, 2308.16903.
- [61] I. Antoniadis and T.N. Truong, Lower Bound for Branching Ratio of $K^+ \to \pi^+$ Axion and Nonexistence of Peccei-Quinn Axion, Phys. Lett. 109B (1982) 67.
- [62] W.A. Bardeen, R.D. Peccei and T. Yanagida, CONSTRAINTS ON VARIANT AXION MODELS, Nucl. Phys. B279 (1987) 401.
- [63] JEF collaboration, L. Gan et al., "Update to the JEF proposal (PR12-14-004)." https://www.jlab.org/exp_prog/proposals/17/C12-14-004.pdf.
- [64] REDTOP collaboration, The REDTOP experiment: Rare η/η' Decays To Probe New Physics, 2203.07651.
- [65] G. Landini and E. Meggiolaro, Study of the interactions of the axion with mesons and photons using a chiral effective Lagrangian model, Eur. Phys. J. C 80 (2020) 302 [1906.03104].
- [66] C. Hanhart, A. Kupśc, U.G. Meißner, F. Stollenwerk and A. Wirzba, Dispersive analysis for $\eta \to \gamma \gamma^*$, Eur. Phys. J. C 73 (2013) 2668 [1307.5654].
- [67] S. Holz, J. Plenter, C.W. Xiao, T. Dato, C. Hanhart, B. Kubis et al., Towards an improved understanding of $\eta \to \gamma^* \gamma^*$, Eur. Phys. J. C 81 (2021) 1002 [1509.02194].
- [68] F. Stollenwerk, C. Hanhart, A. Kupsc, U.G. Meissner and A. Wirzba, *Model-independent approach to eta -> pi+ pi- gamma and eta' -> pi+ pi- gamma, Phys. Lett. B* **707** (2012) 184 [1108.2419].
- [69] B. Kubis and J. Plenter, Anomalous decay and scattering processes of the η meson, Eur. Phys. J. C 75 (2015) 283 [1504.02588].
- [70] C. Hanhart, S. Holz, B. Kubis, A. Kupść, A. Wirzba and C.W. Xiao, The branching ratio $\omega \to \pi^+\pi^-$ revisited, Eur. Phys. J. C 77 (2017) 98 [1611.09359].
- [71] F. Niecknig, B. Kubis and S.P. Schneider, Dispersive analysis of $\omega > 3\pi$ and $\phi > 3\pi$ decays, Eur. Phys. J. C 72 (2012) 2014 [1203.2501].
- [72] JPAC collaboration, $\omega \to 3\pi$ and $\omega \pi^0$ transition form factor revisited, Eur. Phys. J. C 80 (2020) 1107 [2006.01058].
- [73] JPAC collaboration, Khuri-Treiman analysis of $J/\psi \rightarrow \pi + \pi \pi 0$, Phys. Rev. D 108 (2023) 014035 [2304.09736].
- [74] H. Georgi, D.B. Kaplan and L. Randall, Manifesting the Invisible Axion at Low-energies, Phys. Lett. B 169 (1986) 73.

- [75] J. Gasser and H. Leutwyler, Chiral Perturbation Theory: Expansions in the Mass of the Strange Quark, Nucl. Phys. B 250 (1985) 465.
- [76] P. Herrera-Siklody, J.I. Latorre, P. Pascual and J. Taron, Chiral effective Lagrangian in the large N(c) limit: The Nonet case, Nucl. Phys. B 497 (1997) 345 [hep-ph/9610549].
- [77] P. Herrera-Siklody, J.I. Latorre, P. Pascual and J. Taron, Eta eta-prime mixing from $U(3)(L) \times U(3)(R)$ chiral perturbation theory, Phys. Lett. B 419 (1998) 326 [hep-ph/9710268].
- [78] H. Leutwyler, On the 1/N expansion in chiral perturbation theory, Nucl. Phys. B Proc. Suppl. 64 (1998) 223 [hep-ph/9709408].
- [79] R. Kaiser and H. Leutwyler, Large N(c) in chiral perturbation theory, Eur. Phys. J. C 17 (2000) 623 [hep-ph/0007101].
- [80] G. 't Hooft, How Instantons Solve the U(1) Problem, Phys. Rept. 142 (1986) 357.
- [81] H. Leutwyler, Implications of eta eta-prime mixing for the decay eta —> 3 pi, Phys. Lett. B 374 (1996) 181 [hep-ph/9601236].
- [82] R. Escribano, S. Gonzalez-Solis and P. Roig, Predictions on the second-class current decays $\tau^- \to \pi^- \eta^{(\prime)} \nu_{\tau}$, Phys. Rev. D **94** (2016) 034008 [1601.03989].
- [83] KLOE collaboration, Measurement of the pseudoscalar mixing angle and eta-prime gluonium content with KLOE detector, Phys. Lett. B 648 (2007) 267 [hep-ex/0612029].
- [84] X.-K. Guo, Z.-H. Guo, J.A. Oller and J.J. Sanz-Cillero, Scrutinizing the η-η' mixing, masses and pseudoscalar decay constants in the framework of U(3) chiral effective field theory, JHEP 06 (2015) 175 [1503.02248].
- [85] H. Georgi, A bound on m(eta) / m(eta-prime) for large n(c), Phys. Rev. D 49 (1994) 1666 [hep-ph/9310337].
- [86] G. Colangelo, S. Lanz, H. Leutwyler and E. Passemar, Dispersive analysis of $\eta \to 3\pi$, Eur. Phys. J. C 78 (2018) 947 [1807.11937].
- [87] T. Isken, B. Kubis, S.P. Schneider and P. Stoffer, Dispersion relations for $\eta' \to \eta \pi \pi$, Eur. Phys. J. C 77 (2017) 489 [1705.04339].
- [88] T.N. Truong, Chiral Perturbation Theory and Final State Theorem, Phys. Rev. Lett. 61 (1988) 2526.
- [89] A. Dobado, M.J. Herrero and T.N. Truong, Unitarized Chiral Perturbation Theory for Elastic Pion-Pion Scattering, Phys. Lett. B 235 (1990) 134.
- [90] T.N. Truong, Remarks on the unitarization methods, Phys. Rev. Lett. 67 (1991) 2260.
- [91] A. Dobado and J.R. Pelaez, The Inverse amplitude method in chiral perturbation theory, Phys. Rev. D 56 (1997) 3057 [hep-ph/9604416].
- [92] G.F. Chew and S. Mandelstam, Theory of low-energy pion pion interactions, Phys. Rev. 119 (1960) 467.
- [93] J.A. Oller and E. Oset, N/D description of two meson amplitudes and chiral symmetry, Phys. Rev. D 60 (1999) 074023 [hep-ph/9809337].
- [94] J.A. Oller, E. Oset and A. Ramos, Chiral unitary approach to meson meson and meson baryon interactions and nuclear applications, Prog. Part. Nucl. Phys. 45 (2000) 157 [hep-ph/0002193].

- [95] F. Guerrero and J.A. Oller, K\(\bar{K}\) scattering amplitude to one loop in chiral perturbation theory, its unitarization and pion form-factors, Nucl. Phys. B 537 (1999) 459 [hep-ph/9805334].
- [96] S. Gonzàlez-Solís and E. Passemar, $\eta' \to \eta \pi \pi$ decays in unitarized resonance chiral theory, Eur. Phys. J. C 78 (2018) 758 [1807.04313].
- [97] A.M. Badalian, L.P. Kok, M.I. Polikarpov and Y.A. Simonov, Resonances in Coupled Channels in Nuclear and Particle Physics, Phys. Rept. 82 (1982) 31.
- [98] A. Gomez Nicola and J.R. Pelaez, Meson meson scattering within one loop chiral perturbation theory and its unitarization, Phys. Rev. D 65 (2002) 054009 [hep-ph/0109056].
- [99] Z. Xiao and H.-q. Zheng, The Use of dispersion relations in the pi pi and K anti-K coupled channel system, Commun. Theor. Phys. 48 (2007) 685 [hep-ph/0103042].
- [100] T. Ledwig, J. Nieves, A. Pich, E. Ruiz Arriola and J. Ruiz de Elvira, Large-N_c naturalness in coupled-channel meson-meson scattering, Phys. Rev. D 90 (2014) 114020 [1407.3750].
- [101] S.M. Roy, Exact integral equation for pion pion scattering involving only physical region partial waves, Phys. Lett. B **36** (1971) 353.
- [102] JPAC collaboration, Novel approaches in hadron spectroscopy, Prog. Part. Nucl. Phys. 127 (2022) 103981 [2112.13436].
- [103] K.M. Watson, The Effect of final state interactions on reaction cross-sections, Phys. Rev. 88 (1952) 1163.
- [104] K.M. Watson, Some general relations between the photoproduction and scattering of pi mesons, Phys. Rev. 95 (1954) 228.
- [105] R. Omnes, On the Solution of certain singular integral equations of quantum field theory, Nuovo Cim. 8 (1958) 316.
- [106] R. Garcia-Martin, R. Kaminski, J.R. Pelaez, J. Ruiz de Elvira and F.J. Yndurain, The Pion-pion scattering amplitude. IV: Improved analysis with once subtracted Roy-like equations up to 1100 MeV, Phys. Rev. D 83 (2011) 074004 [1102.2183].
- [107] B. Moussallam, N(f) dependence of the quark condensate from a chiral sum rule, Eur. Phys. J. C 14 (2000) 111 [hep-ph/9909292].
- [108] J.F. De Troconiz and F.J. Yndurain, Precision determination of the pion form-factor and calculation of the muon g-2, Phys. Rev. D 65 (2002) 093001 [hep-ph/0106025].
- [109] S. Gonzàlez-Solís and P. Roig, A dispersive analysis of the pion vector form factor and $\tau^- \to K^- K_S \nu_\tau$ decay, Eur. Phys. J. C 79 (2019) 436 [1902.02273].
- [110] M. Albaladejo and B. Moussallam, Extended chiral Khuri-Treiman formalism for $\eta \to 3\pi$ and the role of the $a_0(980)$, $f_0(980)$ resonances, Eur. Phys. J. C 77 (2017) 508 [1702.04931].
- [111] B. Ananthanarayan, I. Caprini, G. Colangelo, J. Gasser and H. Leutwyler, Scalar form-factors of light mesons, Phys. Lett. B 602 (2004) 218 [hep-ph/0409222].
- [112] J.A. Oller and L. Roca, Scalar radius of the pion and zeros in the form factor, Phys. Lett. B 651 (2007) 139 [0704.0039].
- [113] G. Colangelo, E. Passemar and P. Stoffer, A dispersive treatment of $K_{\ell 4}$ decays, Eur. Phys. J. C 75 (2015) 172 [1501.05627].

- [114] J.E. Kim, Weak Interaction Singlet and Strong CP Invariance, Phys. Rev. Lett. 43 (1979) 103.
- [115] M.A. Shifman, A.I. Vainshtein and V.I. Zakharov, Can Confinement Ensure Natural CP Invariance of Strong Interactions?, Nucl. Phys. B166 (1980) 493.
- [116] M. Dine, W. Fischler and M. Srednicki, A Simple Solution to the Strong CP Problem with a Harmless Axion, Phys. Lett. 104B (1981) 199.
- [117] A.R. Zhitnitsky, On Possible Suppression of the Axion Hadron Interactions. (In Russian), Sov. J. Nucl. Phys. 31 (1980) 260.
- [118] J. Liu, N. McGinnis, C.E.M. Wagner and X.-P. Wang, Challenges for a QCD Axion at the 10 MeV Scale, JHEP 05 (2021) 138 [2102.10118].
- [119] D.J. Mack, Physics and outlook for rare, all-neutral Eta decays, EPJ Web Conf. 73 (2014) 03015.
- [120] M. Achasov et al., STCF conceptual design report (Volume 1): Physics & detector, Front. Phys. (Beijing) 19 (2024) 14701 [2303.15790].
- [121] HADES collaboration, I. Ciepal, "Prospects for studies of production, decays and structure of light mesons with hades at precision tests of fundamental physics with light mesons." https://indico.ectstar.eu/event/168/contributions/3667/attachments/2425/3335/iciepal_ECT_june2023.pdf, ECT*, Trento, 2023.
- [122] I. Ciepal. Private communication.
- [123] CMS collaboration, Observation of the rare decay of the η meson to four muons, Phys. Rev. Lett. 131 (2023) 091903 [2305.04904].
- [124] A. Frankenthal and D. Marlow. Private communication.